

Supporting Information

Towards 200 Lumens per Watt of Quantum-Dot White-Light-Emitting Diodes by Reducing Reabsorption Loss

JIA-SHENG LI,^{1,3} YONG TANG,¹ ZONG-TAO LI,^{1,3,*} JIE-XIN LI,¹ XIN-RUI DING,¹ BIN-HAI YU,¹ SHU-DONG YU,¹ JIAN-ZHEN OU,⁴ AND HAO-CHUNG KUO²

¹National & Local Joint Engineering Research Center of Semiconductor Display and Optical Communication Devices, South China University of Technology, Guangzhou 510641, China

²Department of Photonics and Institute of Electro-Optical Engineering College of Electrical and Computer Engineering, National Chiao Tung University, Hsinchu 30010, Taiwan, China

³Guangdong Provincial Key Laboratory of Semiconductor Micro Display, Foshan Nationstar Optoelectronics Company Ltd., Foshan 528000, China

⁴School of Engineering, RMIT University Melbourne, Victoria 3000, Australia

* meztli@scut.edu.cn

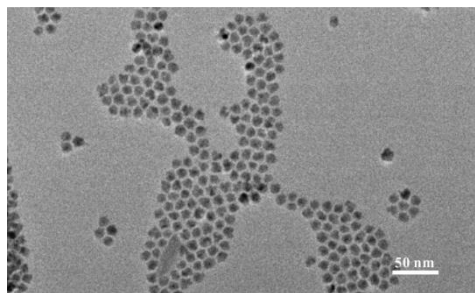


Figure S1. TEM image of green CdSe-based QDs.

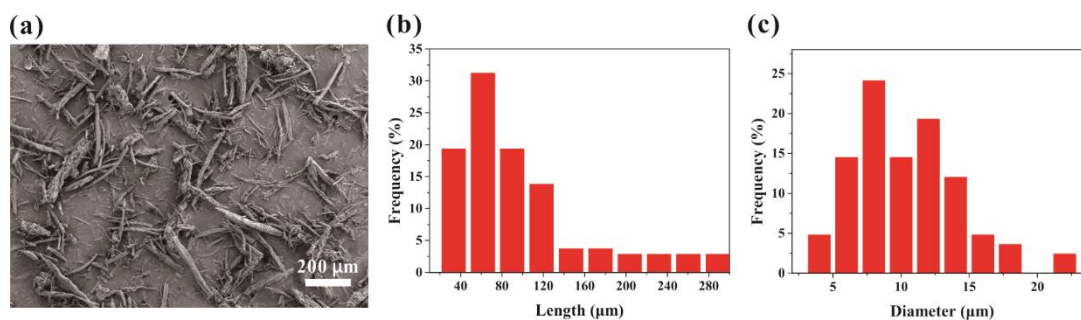


Figure S2. (a) SEM image of SBA-15 particles. (b)-(c) Length and diameter distributions of SBA-15 particles according to 150 samples in the SEM image.

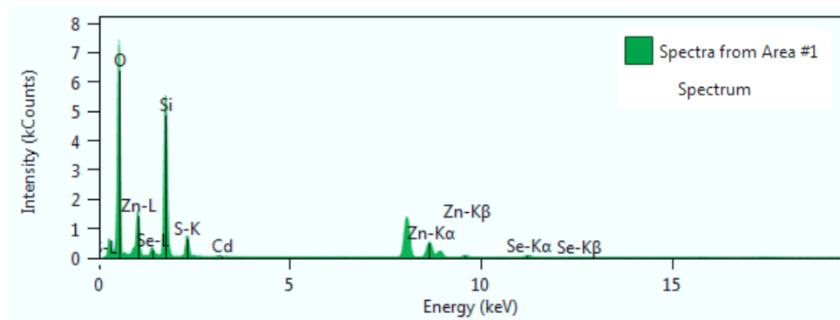


Figure S3. EDS measurement of QD/SBA-15 NPs.

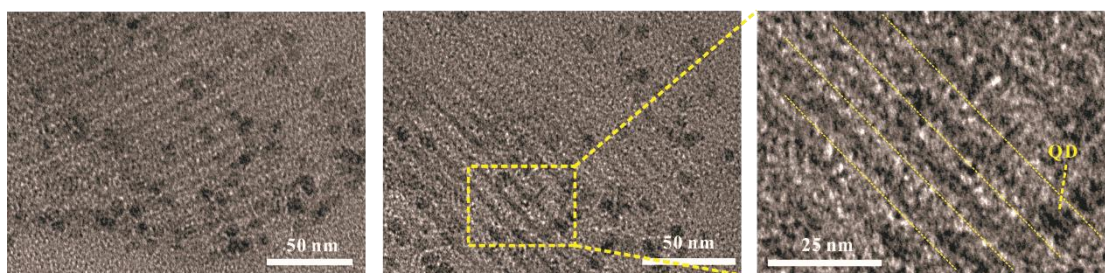


Figure S4. TEM images of the cross-section of a QD/SBA-15 silicone composite. The composite thickness is ~ 60 nm, as obtained from frozen sections. The mass ratio of QDs to SBA-15 particles is 1:5.

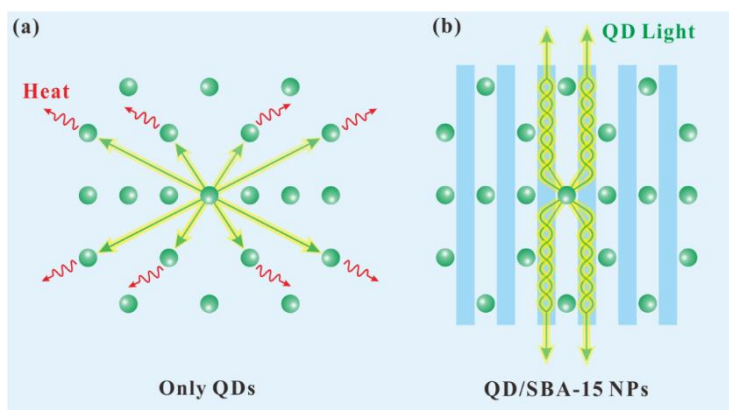


Figure S5. Diagram of the light-extraction mechanisms of QD light. (a) QDs. (b) QD/SBA-15 NPs.

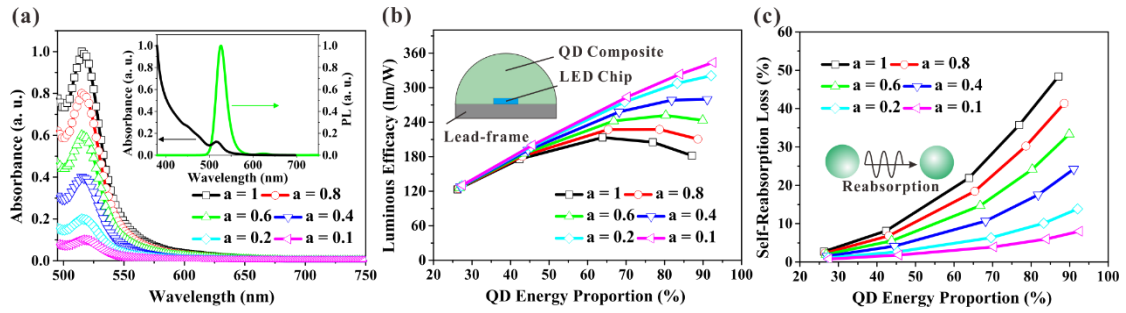


Figure S6. TP simulation of QD white LEDs considering the self-reabsorption loss. (a) Absorbance spectra of QDs with different coefficient a values (the absorbance ratio of QD/SBA-15 NPs to original QDs without adsorption). Absorbance spectrum of $a = 1$ is measured using green QDs and a UV-vis spectrometer (Shimadzu); the inset figure is the photoluminescence (PL) spectrum and absorbance spectrum. (b) The luminous efficacy of QD white LEDs with different values of coefficient a . The insert shows a diagram of the simplified LED device used in the TP simulation. (c) Self-reabsorption loss of QD white LEDs with different values of coefficient a .

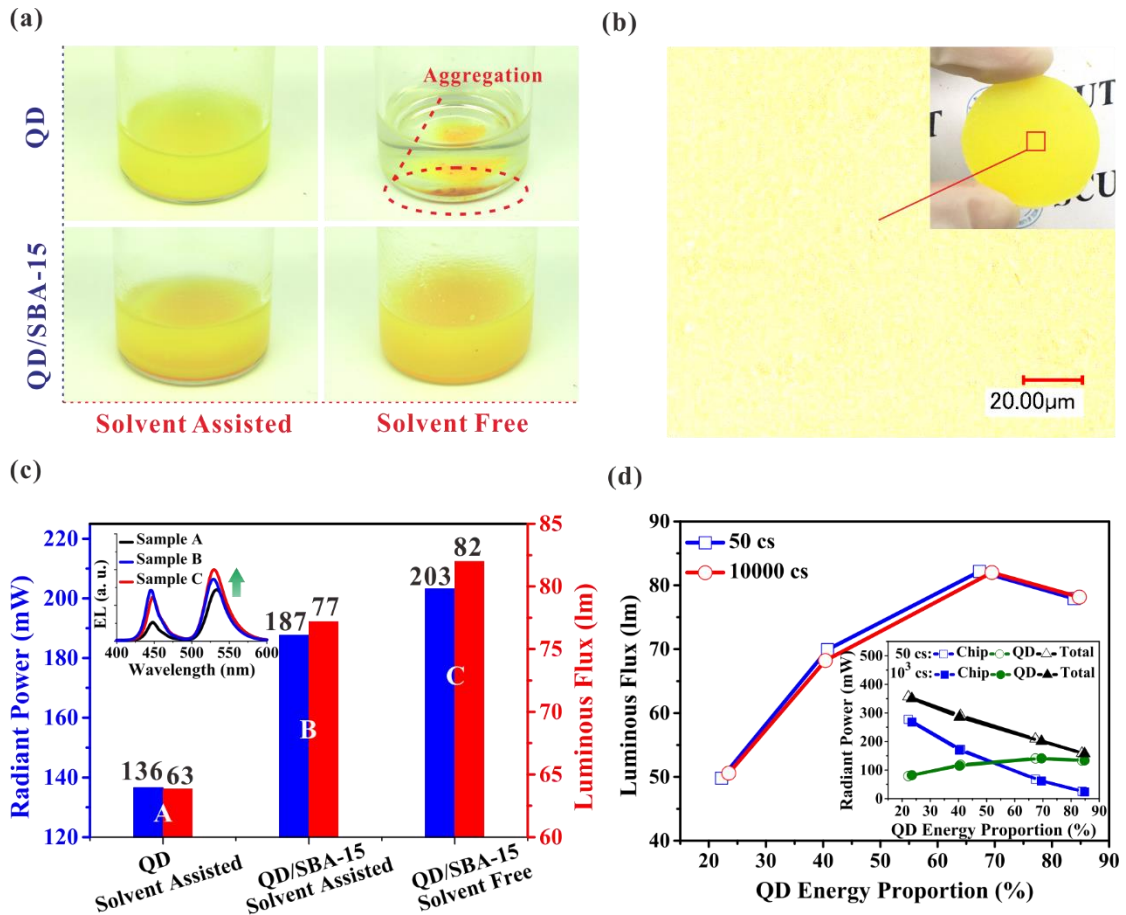


Figure S7. Comparison of the packaging method for QD white LEDs. (a) Photographs of QD composites and QD/SBA-15 composites obtained by the solvent-assisted method and solvent-free

method. (b) Optical microscopy image of the QD/SBA-15 film. (c) The radiant power and luminous flux of QD white LEDs using three different packaging methods. The insert shows the EL spectra of the LEDs. (d) Luminous flux of QD/SBA-15 white LEDs with different viscosities of silicone based on the solvent-free method. The insert shows the radiant power of chip light (from 380 nm to 495 nm), QD light (from 495 nm to 580 nm) and both (the sum of chip light and QD light) for the LEDs, which are calculated according to Figure S9. The QD energy proportion (the ratio of QD light radiant power to total radiant power) is proportional to the QD concentration, as shown in Figure S10. The injection current of these devices is 200 mA.

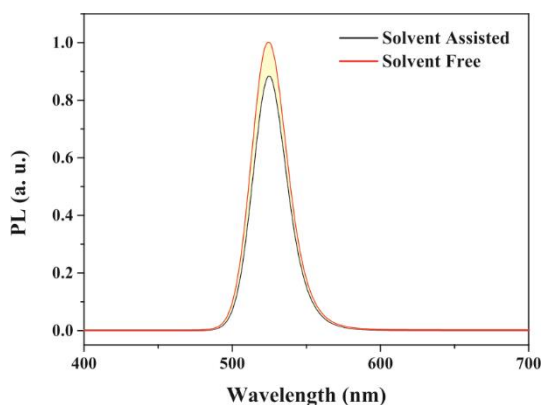


Figure S8. PL spectra of QD/SBA-15 films obtained by the SFP and SAP methods. The QD concentration is 0.8 wt%, the NP mass ratio is 1:5, the film thickness is 1 mm, and the pumping light has a wavelength of 365 nm.

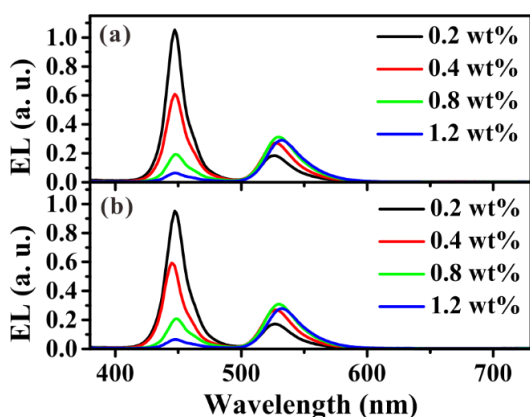


Figure S9. EL spectra of QD/SBA-15 white LEDs with different QD concentrations based on the solvent-free method. The viscosity of silicone is 50 and 10000 cs for (a) and (b), respectively.

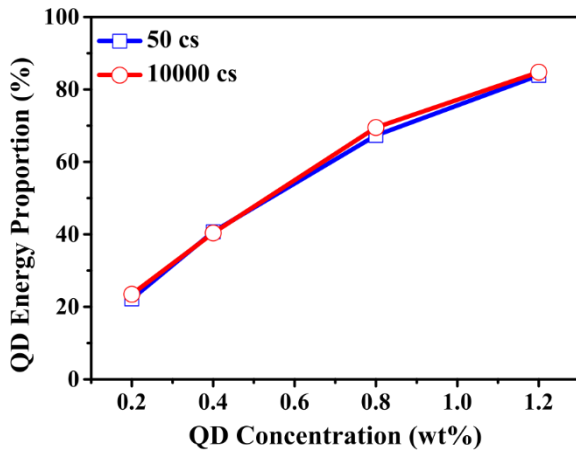


Figure S10. QD energy proportion of QD/SBA-15 white LEDs with different QD concentrations based on the solvent-free method.

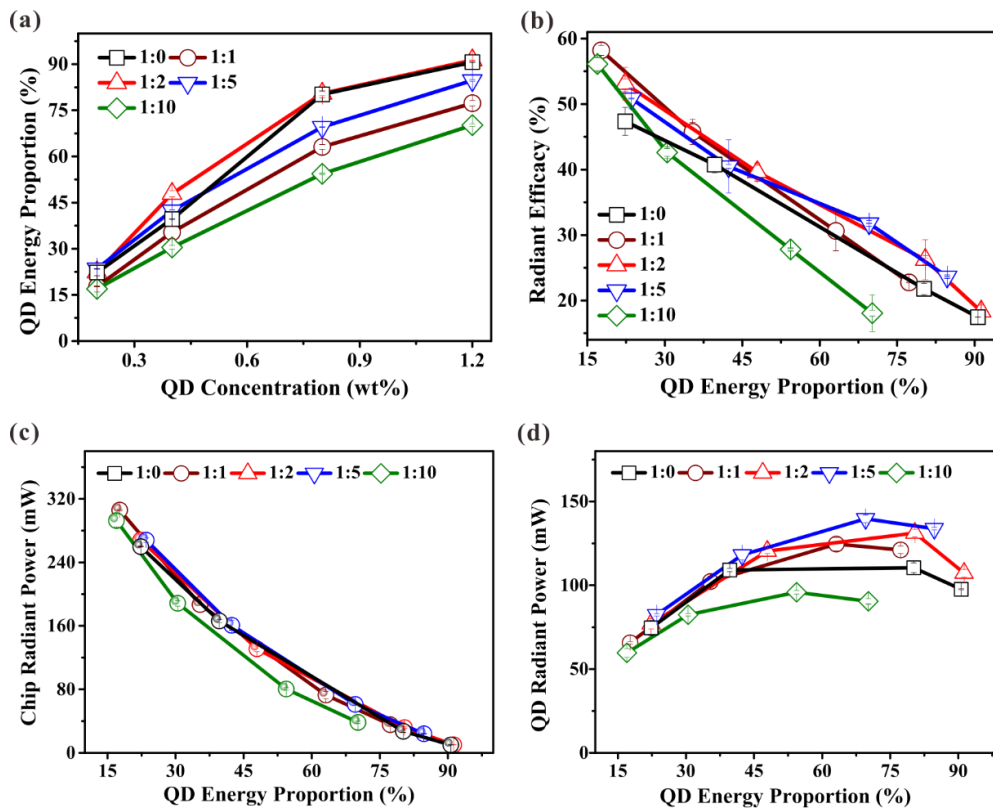


Figure S11. Conversion loss analysis of QD/SBA-15 white LEDs. (a) QD energy proportion of QD/SBA-15 white LEDs at different QD concentrations. (b)-(d) Radiant efficacy, chip radiant power, and QD radiant power of QD/SBA-15 white LEDs at different QD energy proportions. The injection current of these devices is 200 mA.

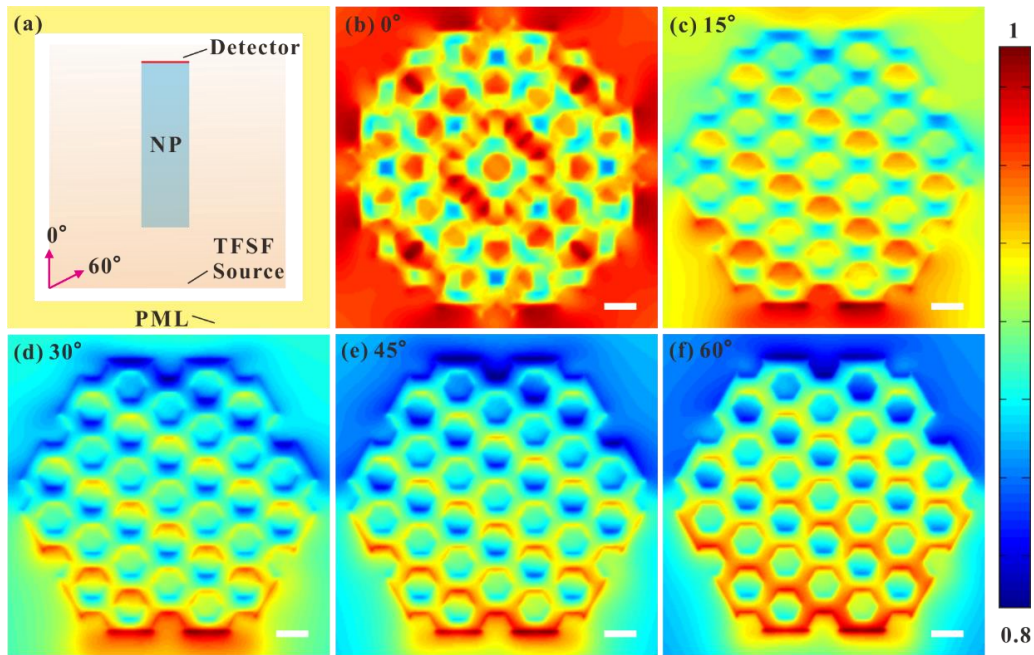


Figure S12. FDTD simulation of SBA-15 particles with different incident angles of blue light (455 nm). (a) FDTD model of SBA-15 particles. The perfected match layer (PML) is set as the boundary condition. The total-field scattered-field (TFSSF) source is set as the source with different incident angles. The detector is set at the top side of the SBA-15 particle to record the electric field. (b)-(f) The electric field of blue light propagating through the SBA-15 particle with incident angles of 0 °, 15 °, 30 °, 45 °, and 60 °, respectively.

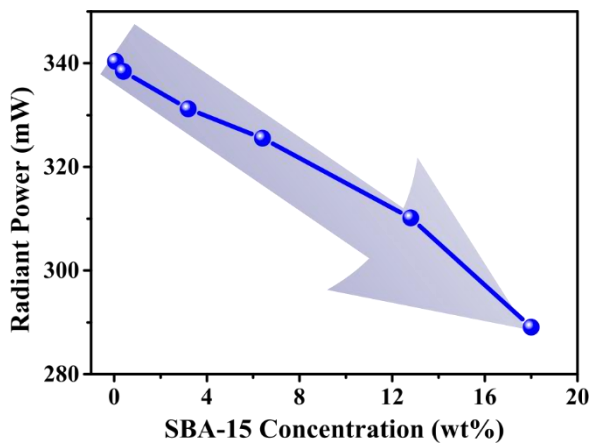


Figure S13. Radiant power of blue LED devices incorporating different concentrations of SBA-15 particles. The injection current is 150 mA.

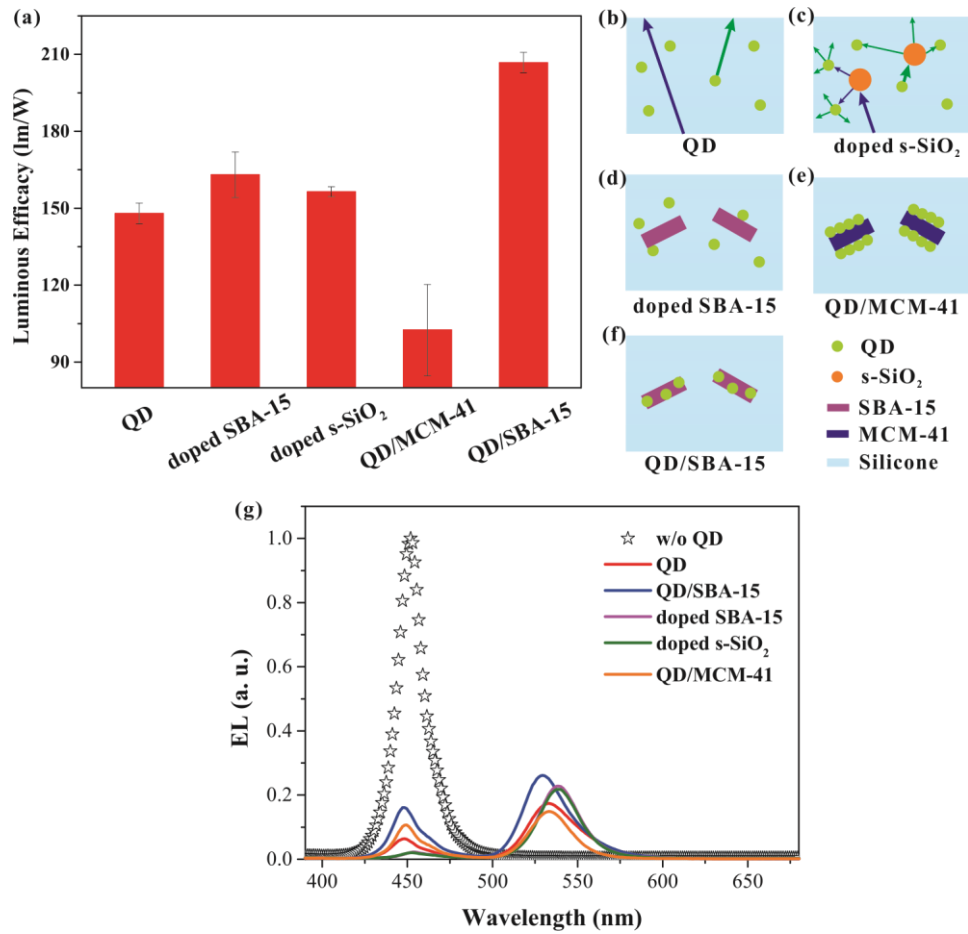


Figure S14. Luminous efficacy of QD white LEDs with different particle structures. (a) Luminous efficacy measured at 20 mA; (b)-(f) diagrams of QD, doped s-SiO₂, doped SBA-15, QD/MCM-41, and QD/SBA-15 structures, respectively; (g) EL spectra measured at 20 mA for references. The green QD concentration is 0.8 wt%, and the mass ratio of QDs to additive particles is 1:5.

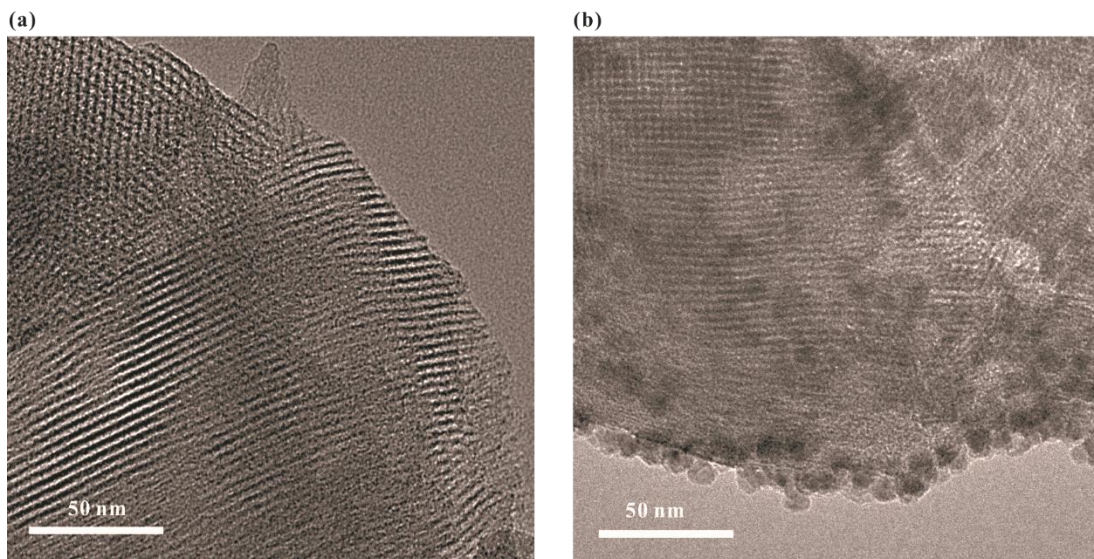


Figure S15. TEM images of (a) MCM-41 particles and (b) QD/MCM-41 NPs. The mass ratio of QDs to MCM-41 particles is 1:5.

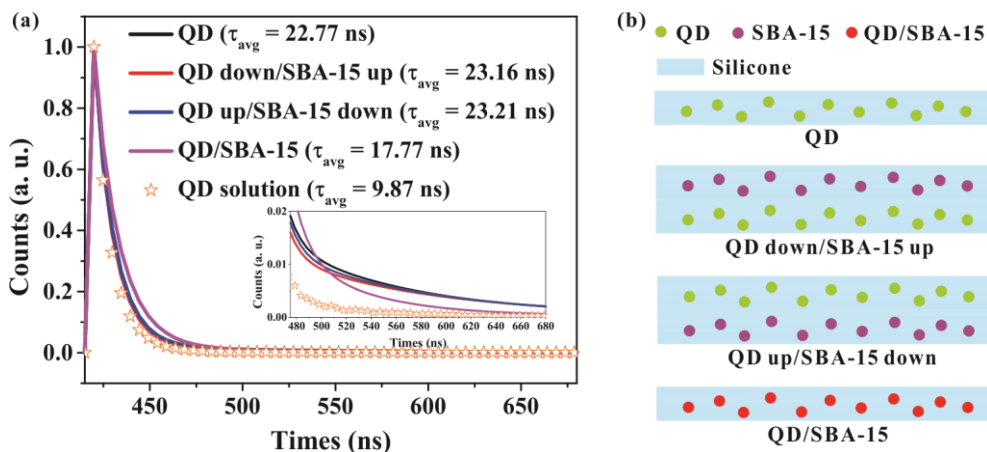


Figure S16. PL lifetime of the QD/SBA-15 silicone composite. (a) PL decay curves; (b) structure diagrams of different silicone composites for comparisons. All of these films have a green QD concentration of 0.8 wt%, and the mass ratio of QDs to SBA-15 particles is 1:5. The green QD solution is used for a reference. The PL decay curves are fitted by the double exponential function to obtain the average PL decay time.

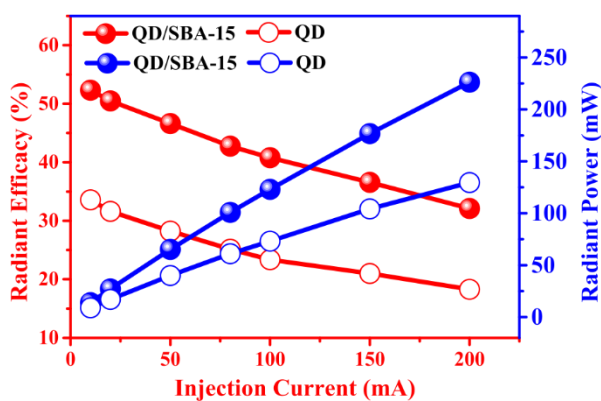


Figure S17. Injection current-dependent radiant efficacy and radiant power of QD/SBA-15 white LEDs. The green QD concentration is 0.8 wt%.

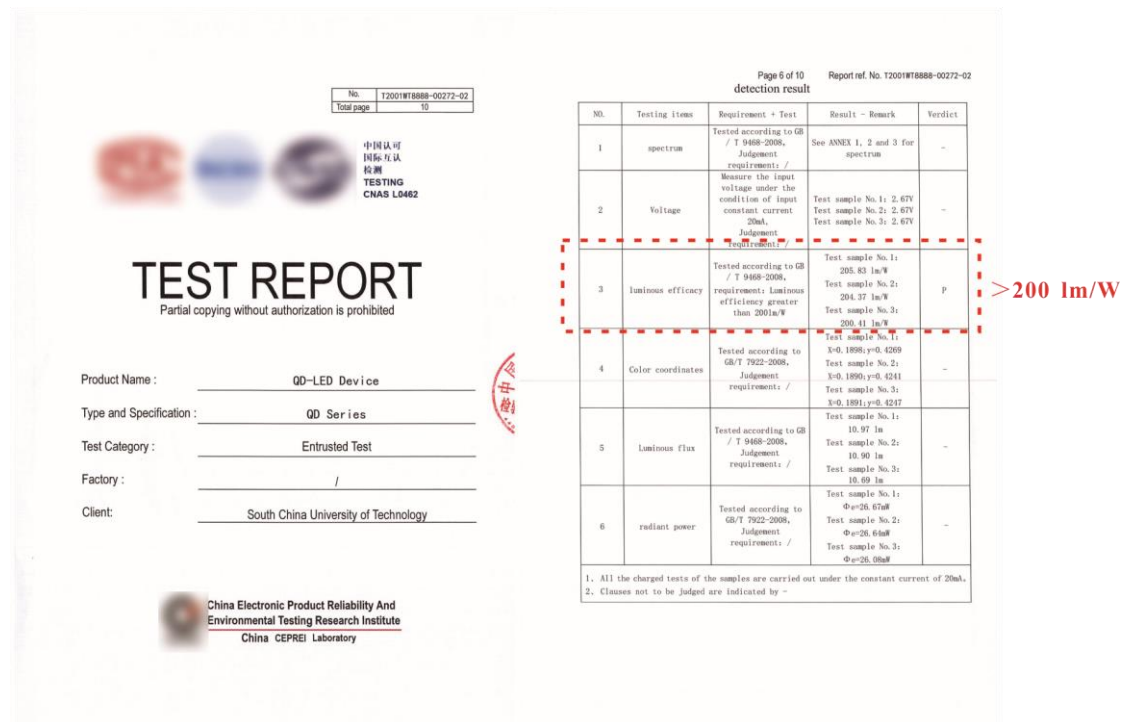


Figure S18. Entrusted test results (certificated by CNAS) of optimized white LEDs using green QDs as the only color convertors.

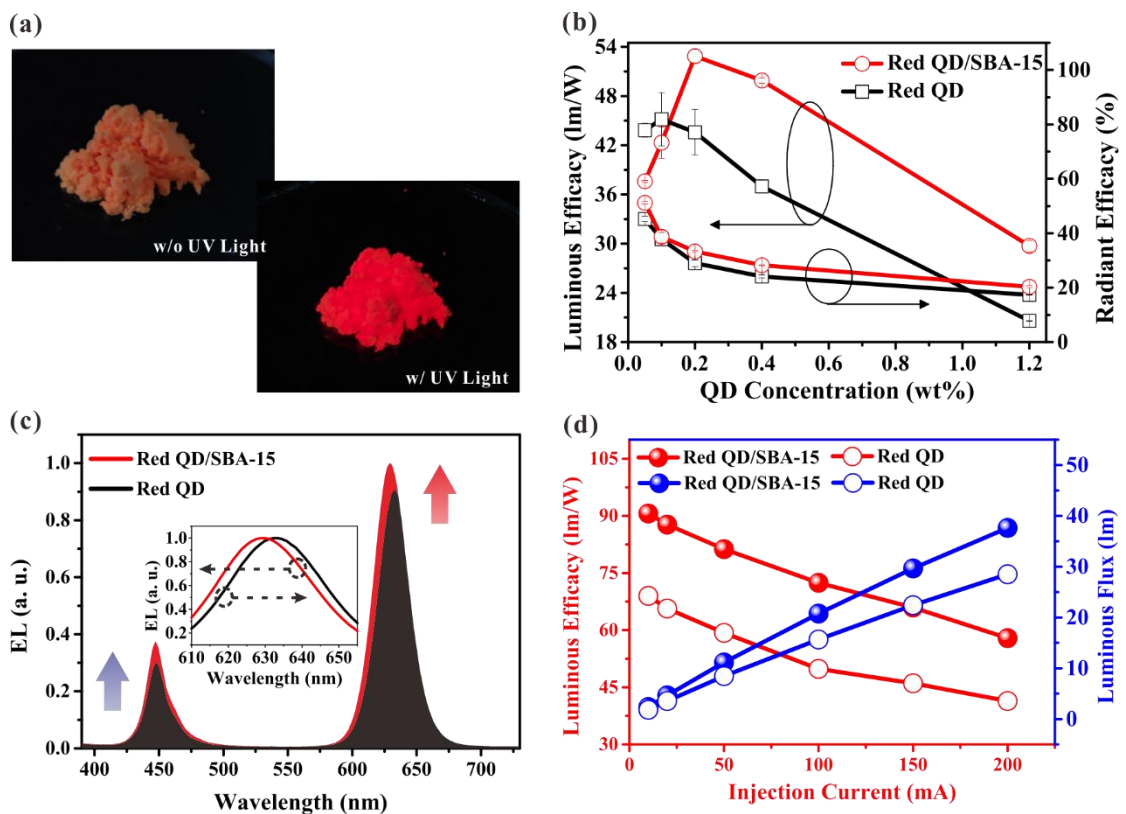


Figure S19. Optical performances of red QD/SBA-15 LEDs using red CdSe-based QDs. (a)

Photographs of red QD/SBA-15 NPs. (b) The luminous efficacy and radiant efficacy of red QD LEDs and red QD/SBA-15 LEDs with different QD concentrations. (c) EL spectra comparison of red QD LEDs and red QD/SBA-15 LEDs. The insert is the normalized EL spectra of the LEDs in the red light range. (d) The injection current-dependent luminous efficacy and luminous flux of red QD LEDs and red QD/SBA-15 LEDs. The injection current for (b)-(c) is 200 mA. The red QD concentration for (c)-(d) is 0.2 wt%.

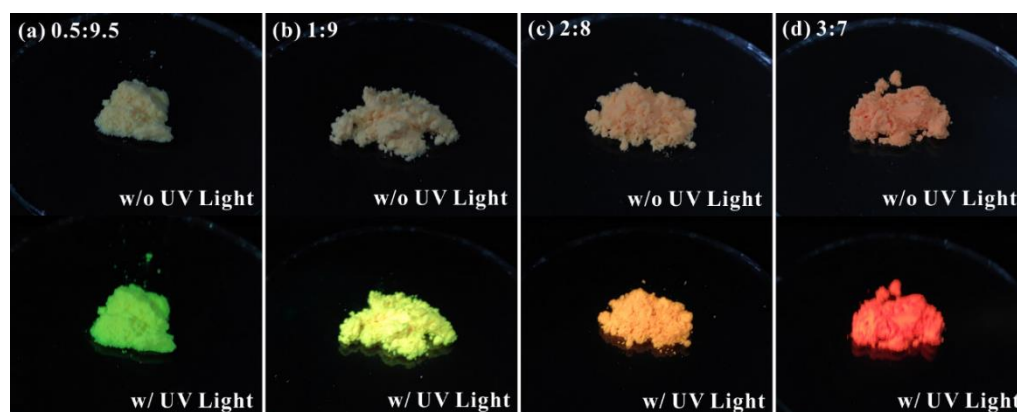


Figure S20. Photographs of RG-QD/SBA-15 NPs with different RG mass ratios. (a)-(d) The RG mass ratios are 0.5:9.5, 1:9, 2:8, and 3:7.

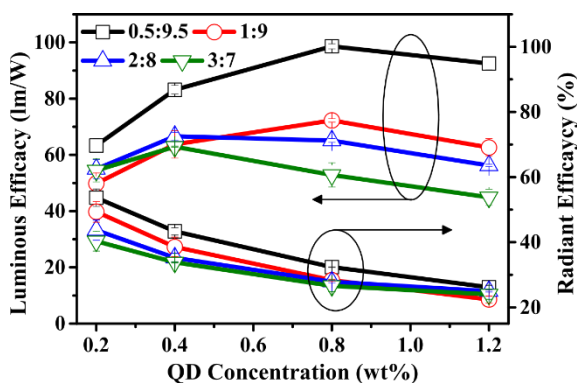


Figure S21. Luminous efficacy and radiant efficacy of RG-QD/SBA-15 white LEDs with different RG mass ratios at various QD concentrations.

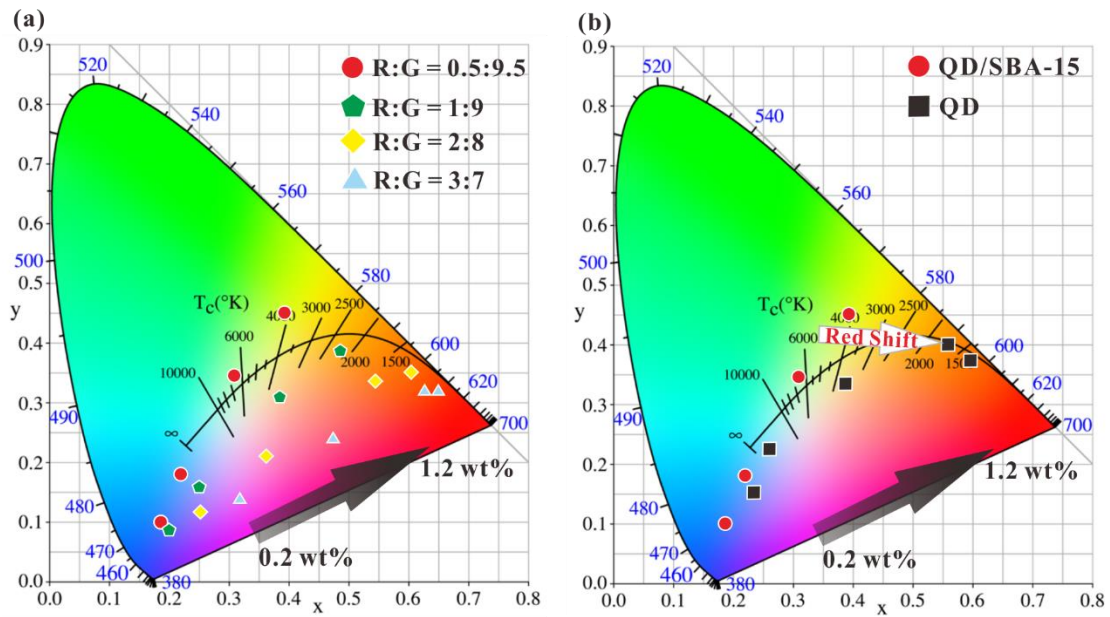


Figure S22. The CIE 1931 color coordinates of wide-color-gamut white LEDs. (a) RG-QD/SBA-15 white LEDs with different RG mass ratios at QD concentrations from 0.2 wt% to 1.2 wt%. (b) RG-QD white LEDs with an RG mass ratio of 0.5:9.5 at QD concentrations from 0.2 wt% to 1.2 wt%.

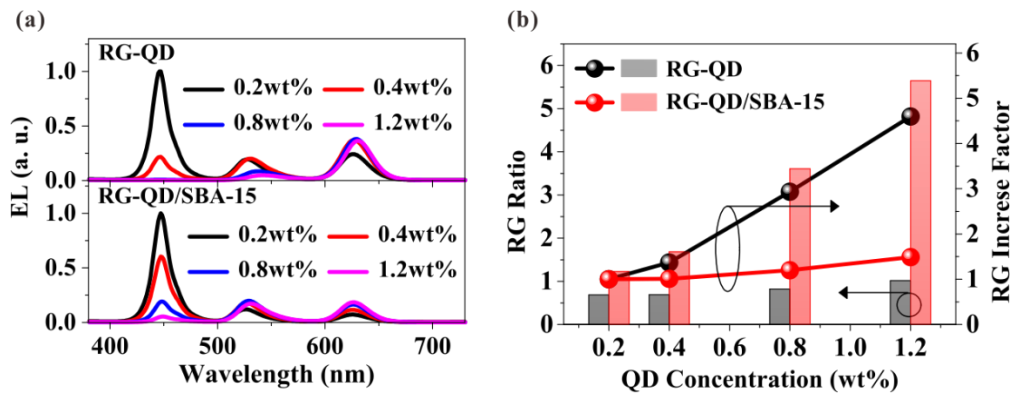


Figure S23. Spectrum analysis of wide-color-gamut QD white LEDs. (a) EL spectra. (b) The RG ratio and RG increase factor.

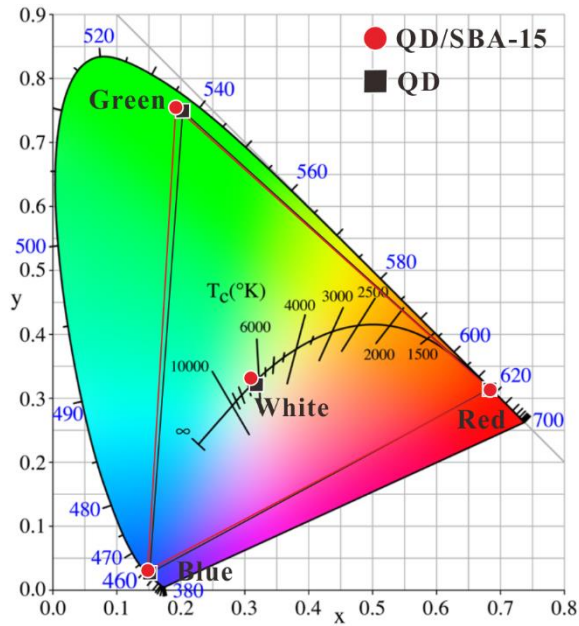


Figure S24. The CIE 1931 color coordinates and triangles of each color component for RG-QD/SBA-15 white LEDs and RG-QD white LEDs with similar color coordinates.

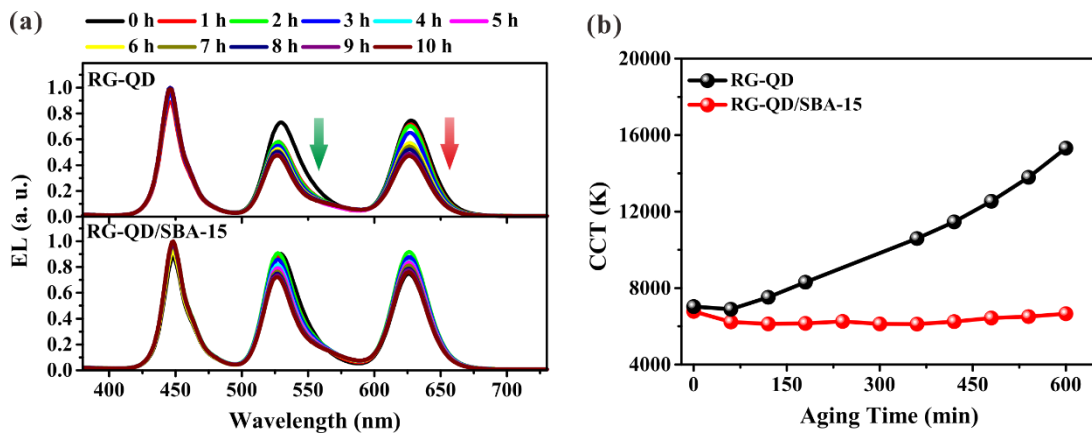


Figure S25. Operating stability of wide-color-gamut white LEDs. (a)-(b) Spectra and CCT of devices after aging for different hours. Aging is set up under harsh conditions in which the injection current is 200 mA, there is no heat sink for efficient heat dissipation, and the environmental temperature is 25 °C.

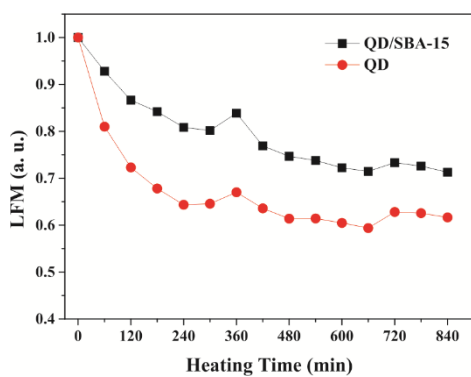


Figure S26. Thermal stability of wide-color-gamut white LEDs. The devices were aged in an oven with a high temperature of 150 °C.

Table S1. The CIE 1931 color coordinates and the color gamut for wide color gamut white LEDs are summarized in Figure S24.

Devices	White	Blue	Green	Red	Color Gamut
QD/SBA-15	(0.3105, 0.3326)	(0.1519, 0.0269)	(0.1940, 0.7547)	(0.6852, 0.3146)	118% NTSC
QD	(0.3181, 0.3230)	(0.1517, 0.0270)	(0.2043, 0.7493)	(0.6850, 0.3148)	116% NTSC

Table S2. Thermal conductivity of a QD silicone composite and QD/SBA-15 silicone composite measured by the transient plane source method (Hot Disk TPS2500S, Sweden). The green QD concentration is 0.8 wt%, and the mass ratio of QDs to SBA-15 particles is 1:5.

Sample	Measurement Temperature (°C)	Thermal Conductivity (W/m K)
QD silicone composite	25	0.3209
QD/SBA-15 silicone composite		0.3948